NANO LETTERS

pubs.acs.org/NanoLett

Graphene Islands on Cu Foils: The Interplay between Shape, Orientation, and Defects

Joseph M. Wofford,[†,‡] Shu Nie,[§] Kevin F. McCarty,[§] Norman C. Bartelt,[§] and Oscar D. Dubon*[,†,‡]

[†] Department of Materials Science and Engineering, University of California, Berkeley, California 94720, United States, [‡] Materials Sciences Division, Lawrence Berkeley National Laboratory, Berkeley, California 94720, United States, and [§] Sandia National Laboratories, Livermore, California 94550, United States

ABSTRACT We have observed the growth of monolayer graphene on Cu foils using low-energy electron microscopy. On the (100)-textured surface of the foils, four-lobed, 4-fold-symmetric islands nucleate and grow. The graphene in each of the four lobes has a different crystallographic alignment with respect to the underlying Cu substrate. These "polycrystalline" islands arise from complex heterogeneous nucleation events at surface imperfections. The shape evolution of the lobes is well explained by an angularly dependent growth velocity. Well-ordered graphene forms only above ~790 °C. Sublimation-induced motion of Cu steps during growth at this temperature creates a rough surface, where large Cu mounds form under the graphene islands. Strategies for improving the quality of monolayer graphene grown on Cu foils must address these fundamental defect-generating processes.

KEYWORDS Graphene, copper, epitaxy, low-energy electron microscopy, low-energy electron diffraction

The unique electronic structure[1] and exceptional structural quality of graphene leads to exciting room-temperature properties such as the quantum Hall effect[2] and an electron mobility of 120000 $cm^2/(V\ s)$.[3] The majority of investigations have used graphene obtained by micromechanical cleavage,[4] which is not amenable to commercial applications. Graphene can also form during the thermal decomposition of SiC,[5−7] by the surface segregation of C dissolved in metal substrates,[8−10] and by decomposition of hydrocarbons on metals.[11,12] Further refining these alternative production techniques is crucial if graphene is to become a technologically relevant material.

In particular graphene growth on Cu foils has shown great promise as a source of large area, monolayer graphene.[13] The low solubility of C in Cu is believed to self-limit graphene growth to monolayers.[14] However, despite its potential, little is known about the factors that control graphene quality, such as nucleation and growth kinetics, on Cu foils. Indeed, even how graphene is aligned with the Cu remains an open question.

Using low-energy electron microscopy (LEEM) to observe graphene growth in situ, we shed light on these critical issues. The surfaces of the Cu foils are strongly (100)-textured. We discover that graphene grows on this surface in a strikingly different mode than on the close-packed surfaces of other metals.[8−12] Each graphene island has a prominent four-lobed morphology that persists until interrupted by interisland impingement or by Cu surface imperfections. Each lobe of a graphene island has a different rotation about the film normal. By measuring growth velocities, we find this structure arises from growth dominated by edge kinetics with an angularly dependent growth velocity. Unfortunately at the temperatures required to synthesize graphene, considerable Cu sublimation occurs. This, as we show, roughens the Cu surface and, thus, the conformal graphene film.

Graphene was grown on 25 μm thick polycrystalline Cu foil (Johnson Matthey, 99.999% Cu, catalogue #10950). Prior to deposition, the Cu foil was annealed in a tube furnace at 1000 °C for ~45 min in an $Ar-H_2$ mixture at atmospheric pressure. Samples were transferred in air to a LEEM having a base pressure of $\sim 1 \times 10^{-10}$ Torr, where graphene was grown. The temperatures quoted below were obtained from a thermocouple welded to the sample holder; comparison with the observed melting point of the foils suggests the sample temperature is underestimated by 80−100 °C. In the LEEM the foils were annealed at ~960 °C for 10 min and subsequently cooled to the growth temperature, which ranged from about 740 to 895 °C.

Pregrowth low-energy electron diffraction (LEED) analysis of the Cu surface shows that this annealing results in a (100) texture in the foil plane. The Cu LEED pattern was still detectable after graphene growth (Figure 1a). The (100) texture is characteristic of Cu foils made by cold rolling and recrystallized by subsequent annealing.[15] The surfaces of many grains were very precisely aligned with the (100) plane. The spacings between single Cu atomic steps were often greater than 100 nm, indicating surface normals less than 0.1° from the [100] azimuth. This degree of alignment rivals or exceeds the surfaces typically obtained by cutting and polishing single crystals. Cu grain sizes were observed

* Corresponding author, oddubon@berkeley.edu.
Received for review: 08/7/2010
Published on Web: 10/27/2010

DOI: 10.1021/nl102788f | *Nano Lett.* **2010,** *10,* 4890–4896

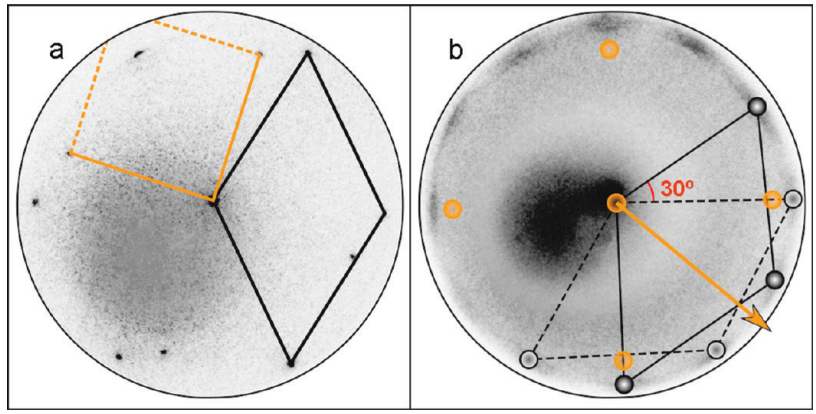

FIGURE 1. A LEED pattern of a single graphene lobe on Cu(100) (a), with the reciprocal unit cell of the graphene (black) and the reciprocal surface unit cell of the Cu (orange) shown. Notice the sharpness of the 6-fold graphene pattern, indicating good crystallinity, and that the 4-fold Cu pattern is simultaneously observed. When many graphene crystals are simultaneously probed a diffuse LEED pattern develops, composed of 12 arcs, each spanning ~15° (b). The reciprocal unit cells of the two equivalent graphene orientations are shown (see black and dashed diamonds, orange dots are the Cu pattern). Notice that the Cu(100) direction (orange arrow) falls at the approximate midpoint of the two graphene orientations.

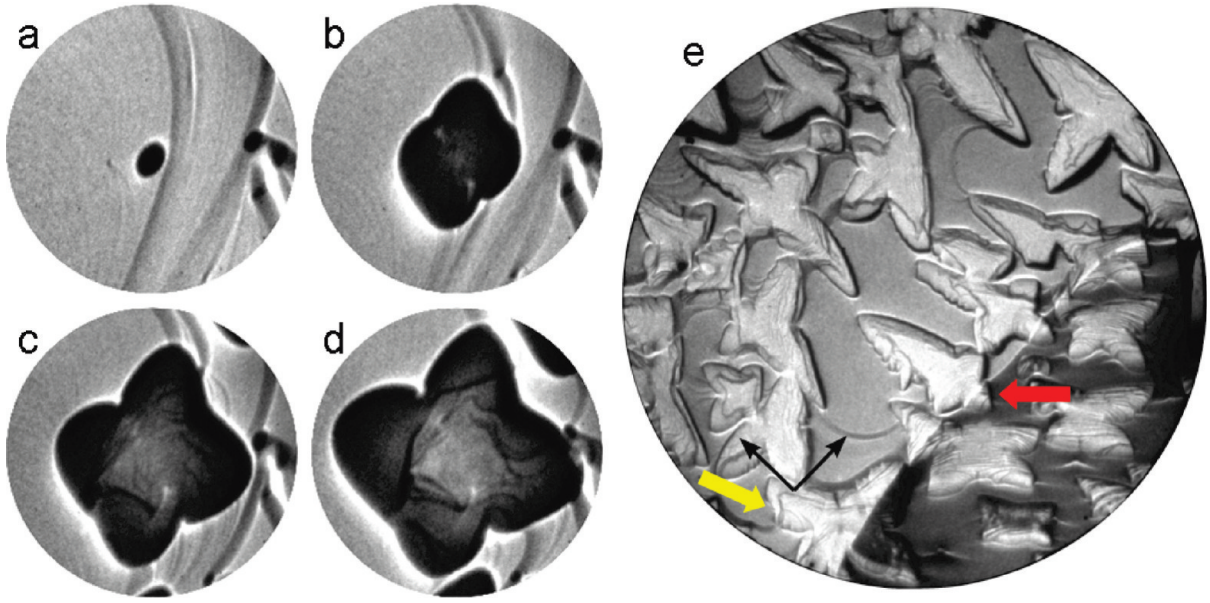

FIGURE 2. LEEM images of the evolution of a graphene island on Cu(100) at 842 °C after (a) 15 s of C deposition, (b) 90 s, (c) 240 s, and (d) 390 s (FOV = 10 μm). This process results in distinctly four-lobed islands (e). The axes of the graphene lobes tend to align along Cu⟨001⟩ directions (black arrows). Graphene lobes are able to grow across Cu grain boundaries (red arrow) and can be distorted by large Cu step bunches (yellow arrow, FOV = 46 μm, grown at 790 °C).

to be as large as ~1 mm with some subgrain annealing twins also present.

Carbon was evaporated from an electron-beam heated graphite rod mounted in the LEEM chamber. (Exposure of the foils to ethylene at pressures below 10^{-7} Torr did not lead to appreciable C adsorption.) We found that a minimum substrate temperature of ~790 °C was necessary to obtain ordered graphene, as characterized by the LEED pattern in Figure 1a with sharp graphene diffraction spots. Deposition at lower temperature yielded C films that did not give graphene diffraction spots. The in-plane orientation of the graphene lattice relative to the Cu lattice varies as we discuss below.

Figure 2a–d shows the nucleation and growth of a representative graphene island. Such islands nucleate heterogeneously at bunches of Cu steps, pinning sites, and other surface imperfections. Initially the graphene island is compact in shape. With time it becomes increasingly ramified, developing a lobed structure. Islands reach a steady-state shape with four branches, and allowing for irregularities, this shape is eventually attained by every graphene island. Figure 2e shows that the long axes of the four graphene lobes are oriented approximately the same from island to island and are usually close to Cu ⟨001⟩ in-plane directions although substantial variations are observed. Graphene lobes were able to grow across Cu grain boundaries (Figure 2e, red

DOI: 10.1021/nl102788f | Nano Lett. 2010, 10, 4890–4896

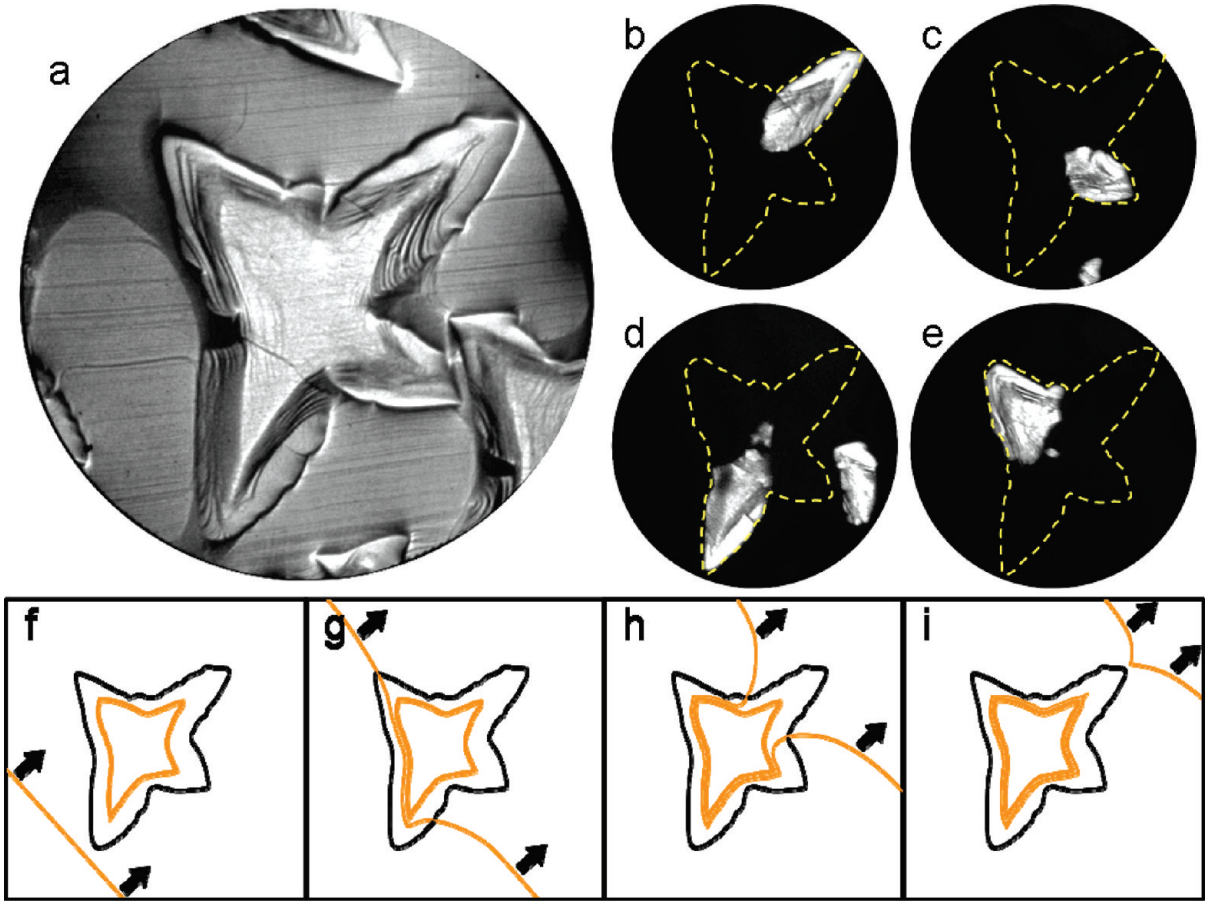

FIGURE 3. Bright (a) and dark field (b−e) LEEM images of a large graphene island on Cu(100) showing the spatial distribution of rotational variants. The graphene (01) direction is rotated by (b) 28°, (c) 2°, (d) 8°, and (e) 42°, relative to Cu(001) (FOV = 20 μm, yellow dashes are the approximate island boundary). Cu step edge accumulation during growth results in a Cu hillock beneath the graphene island, as can be seen in (a). The hillock formation process is illustrated in (f−i).

arrow), although the growth velocity usually drops on crossing the grain boundary. Despite their ramified shape, the graphene islands eventually combine to form a complete polycrystalline film. However, the spaces between islands fill slowly after island impingement occurs.

Why the graphene islands have four lobes is puzzling. According to the Wulff construction,[16] island shapes dictated by edge-energy minimization must have a concave shape, which is contrary to the observed islands. A clue is provided by a diffraction analysis of individual graphene islands. Selected-area diffraction from each lobe of individual islands shows that the islands are not composed of a single orientation of graphene. Instead each lobe is rotated differently about the surface normal. Dark-field LEEM images from first-order graphene diffraction spots in Figure 3b−e reveal the spatial distribution of the rotational variants. Each constituent crystal comes together at the approximate geometric center of the island, suggesting that they share the same nucleation site, consistent with the growth sequence observed in Figure 2. A few islands have a more complicated distribution of rotational variants, perhaps as a result of multiple, spatially close nucleation events.

The highly anisotropic elliptical shape of individual lobes, as shown in Figure 2e, is remarkable. A fundamental question is whether this lobe shape is determined by minimizing edge energy or whether it is a consequence of growth kinetics. This issue can be addressed by monitoring the profile of a lobe as a function of time. In the simplest kinetic model, growth rate is solely a function of orientation. As shown by Frank,[17] systems with an angularly dependent growth velocity exhibit a characteristic behavior. Consider a given point on the crystal edge, defined by its particular edge normal. As the crystal edge advances, the succession of points with the same edge normal will follow a linear trajectory. Figure 4 presents a sample of this type of analysis for a lobe that grew unperturbed by neighboring islands or surface imperfections. Each orientation of this lobe's growth front moves along a line as the lobe tip propagates over a distance of 8.5 μm. This behavior was found for the 12 other freely growing lobes analyzed at ~790 °C. The linearity of the growth trajectory over a substantial range of island sizes demonstrates that a well-defined angularly dependent growth velocity exists for each lobe.

DOI: 10.1021/nl102788f | *Nano Lett.* **2010,** *10,* 4890–4896

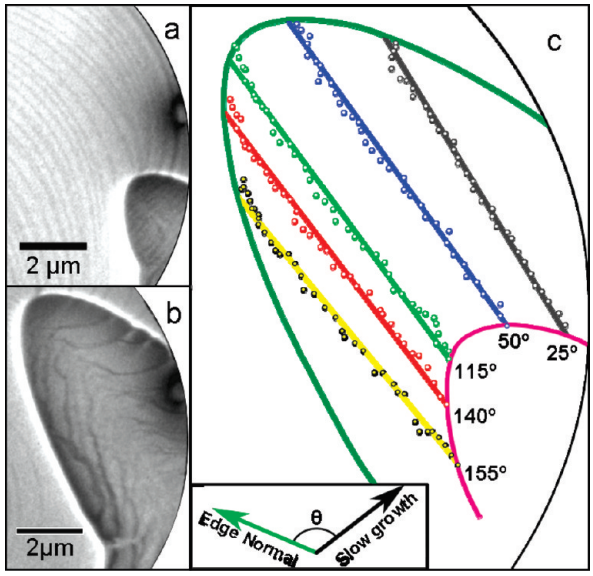

FIGURE 4. A graphene lobe (a) on Cu at 790 °C, and the same lobe 820 s later (b). These lobes are outlined in (c) in purple and dark green, respectively. A growth rate that is solely a function of orientation will result in a linear growth trajectory for a point on the crystal edge with a given normal, as shown in (c) for five points defined by normals of 25° (gray), 50° (blue), 115° (green), 140° (red), and 155° (yellow) relative to the slow-growth direction. As the graphene lobe grew, the location of the points on its edge with these normals was tracked in discrete increments (colored dots, solid lines are linear best-fits). The excellent agreement between the data and fits demonstrates the linearity of the growth trajectories for given graphene edge orientations.

These growth kinetics eventually yield a steady-state shape for each lobe than can be determined from a Wulff construction, with the angularly dependent growth velocity substituting for the surface-energy anisotropy.[17] To see what sort of anisotropy is required to generate the observed shapes, we examine a simple model of growth velocity. For a 6-fold symmetric crystal growing on a 4-fold symmetric substrate, in general the growth velocity will have 2-fold symmetry. A simple 2-fold symmetric model is

$$v(\theta) = (1 + r) + (r - 1)\cos(2\theta)$$

where v is the growth velocity, θ is the angle of the edge normal relative to the slow-growth direction, and r is the ratio of the velocities in the slow and the fast directions. Fitting this model to the graphene island morphology shown in Figure 5 gives $r = 0.25 \pm 0.02$. Notice such a large anisotropy in the model predicts that a sharp tip should develop at the apex of the lobe, as indeed seen in Figure 5. Such sharp tips are evident on many of the lobes seen in Figure 2e. The fitted anisotropy factor is approximately the same for many islands, as seen by the consistent ~2:1 aspect ratio of the lobes in Figure 2e. This anisotropy agrees with the direct measurements of growth velocity shown in Figure 4. In fact, the model predicts growth velocities

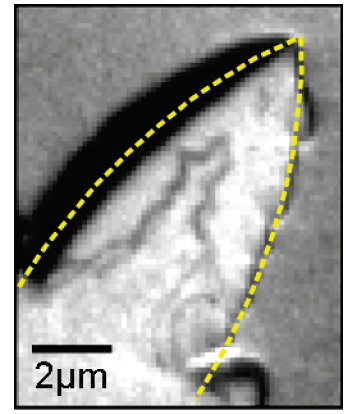

FIGURE 5. The profile of this graphene lobe is well explained by the proposed 2-fold symmetric growth velocity with an anisotropy factor of 0.25 (dashed yellow line is a fit).

involved in determining island shape to within 6%. The validity of this simple model demonstrates that a 2-fold-symmetric angularly dependent growth velocity determines the distinctive shape of the graphene lobes on Cu(100).

The 2-fold symmetry of the growth velocity has interesting implications concerning the factors that influence the graphene growth rate. If growth was dominated by either the graphene itself or the Cu(100) substrate, we would expect 6- or 4-fold symmetry, respectively. The observed 2-fold velocities show that the symmetries of both the Cu and graphene influence growth. Therefore, the growth velocity must also depend on the relative orientation of the two materials. As mentioned above we observe a range of relative in-plane orientations. So what is the interplay between the growth velocity and the orientation? To probe what orientations exist, we recorded a LEED pattern from a 20 μm region containing many graphene islands. As shown in Figure 1b, rather than having sharp graphene spots, this LEED pattern is composed of 12 diffuse arcs. The 12 diffraction arcs arise from the two equivalent ways 6-fold graphene can be aligned with respect to the 4-fold Cu substrate. Their existence establishes that the graphene is not confined to discrete in-plane orientations. Instead, graphene is smeared over about a ±7.5° range of orientations.

As previously shown in Figure 2e, the long axes of the graphene lobe are most-often aligned along Cu⟨001⟩ directions but significant variations exist. The orange arrow in Figure 1b shows one such fast-growth Cu⟨001⟩ direction. Notice that this direction is not aligned with the high-symmetry directions of graphene. Instead Figure 1b shows that the graphene reciprocal lattice is rotated on average about 15° from alignment with Cu⟨001⟩ directions. This yields a sheet whose fast-growing edge is approximately half way between the high-symmetry zigzag and armchair edge structures. If graphene is rotated precisely 15° from Cu⟨001⟩ directions, the edge termination is half zigzag and half armchair. Then the edge termination in the slow- and fast-growth directions, which differ by 90° rotation, would be the same, contrary to observations. But there is no reason

DOI: 10.1021/nl102788f | *Nano Lett.* **2010,** *10,* 4890–4896

from symmetry for the orientation to be precisely half way and any small deviation from this position recovers the 2-fold angular dependence of the velocity. The often-observed deviations of the fast direction away from the ⟨001⟩ Cu directions also restore the 2-fold symmetry.

Orientation is not the only factor determining velocity. Growth rates are also affected by inhomogeneities on the surface. As the growth front intersects pinning sites or approaches an adjacent graphene island, its trajectory is deflected. Additionally, while single Cu step edges do not have a perceptible effect on the growth, large bunches are observed to distort island evolution by altering growth trajectories (see yellow arrow in Figure 2e). These effects may account for the significant lobe-to-lobe variations from the average orientations discussed above. For example, the fast growth is not always precisely along a Cu⟨001⟩ direction. It be as many as 20° away as witnessed by the non-90° angles between some lobes in Figure 3. As shown by the diffuse arcs in Figure 1b, the alignment of graphene with respect to the Cu can also vary by several degrees. In the island analyzed in Figure 4 the fast growth direction relative to the graphene was 6° from the midpoint discussed above, rotated toward the armchair edge termination.

The minimum temperature of ∼790 °C required to grow graphene is sufficiently high to induce significant motion of Cu steps due to Cu sublimation. The Cu step edges interact with pinning sites, grain boundaries, and the growing graphene itself, yielding a constantly evolving Cu morphology. Before growth, the surface of each Cu grain consists of a propagating array of monolayer-height steps. After growth Figures 2e and 3a show that large Cu hillocks now exist underneath the graphene islands. The schematic in Figure 4f−i sketches the hillock creation process. (For a video of the evolution, see the Supporting Information.) When a segment of a Cu step edge collides with a graphene island, it decelerates. Thus, Cu step edges become bunched under the graphene. We attribute the deceleration to Cu atoms that must diffuse laterally from the interior of a graphene island to its edge, onto the exposed Cu surface, in order to sublime. Because these step bunches move relatively slowly underneath graphene, they are unable to flow through the island before additional Cu steps impinge upon them. As a consequence incoming steps wrap around under the interior of the lobed graphene island. Each wrapped step lowers the adjacent, bare Cu by an atomic step spacing relative to the graphene-covered region. This process creates four-lobed Cu hillocks draped by graphene. The hillocks are even more prominent on samples grown at higher temperatures. Indeed, surface roughening can be so dramatic that individual hillocks are easily visible with an optical microscope. As the graphene islands begin to coalesce, Cu step flow is increasingly inhibited.

Unlike reports on other graphene−metal systems (e.g., graphene−Ni and −Ru), we found no evidence of graphene growth by C precipitation from the bulk of the Cu foil. Growth by C segregation usually occurs during sample cooling as the equilibrium solubility of C in the metal drops. It has been implicated in the formation of thicker graphitic films, rather than the desired monolayer.[18] Because C solubility in Cu is relatively low, C segregation to the Cu surface is expected to be small. To confirm this prediction, graphene films of approximately 0.5 monolayer coverage were cycled between ∼700 and ∼950 °C while continuously imaged using LEEM. No C precipitation or island growth was observed during cooling. This is in agreement with recent reports suggesting the process of growing graphene on Cu is confined to the surface, with dissolution and precipitation of C from the substrate not playing a significant role.[14] (Upon heating, the graphene islands shrank slightly. Given the absence of any sign of C segregation on cooling, the source of this effect is not clear. We note that the shrinkage occurred at temperatures that gave very high rates of Cu sublimation.)

The four-lobed structure of the islands likely evolves from a complex nucleation event that simultaneously seeds multiple graphene crystals of different orientations relative to the Cu substrate. Subsequent growth must be outward from the nucleation center. Those graphene crystals that are oriented with a favorable growth condition expand more rapidly than their disadvantaged neighbors, quickly coming to dominate the island structure.

Previous work has shown that carbon monomers diffusing on a metal surface face a large energetic barrier for attachment to graphene.[19] This barrier may depend sensitively on the relative orientation of the graphene and Cu, perhaps because the energy to detach a C monomer from the Cu and attach it to the graphene is heavily influenced by the relative positions of the graphene and the monomer binding site. Alternatively, if the graphene *edge* is strongly bound to the Cu substrate, attachment of monomers would require locally detaching the edge from the substrate. This would also create a barrier that would depend on the alignment of the graphene edge with the substrate.

We note that growth strongly prefers particular edge orientations for a given relative orientation of graphene with respect to Cu. However, there is no strongly preferred relative orientation. This suggests that the interaction between the graphene, away from its edge, and the Cu substrate is relatively weak compared to other graphene−metal systems, like Ru(0001) where only one relative orientation is observed. Rather, the weaker interaction between graphene and Cu suggests that the bonding is similar to the graphene−Pt system.[20] This conclusion is corroborated by Raman spectroscopy. Results in the literature of graphene still supported on the Cu substrate, as well as spectra collected in this investigation (see Supporting Information), show the characteristic G and 2D Raman peaks of graphene.[21] In addition, the peaks are not substantially shifted from the values for free-standing graphene, suggesting that the substrate imposes little strain on the graphene despite substantial differential film/substrate contraction

DOI: 10.1021/nl102788f | *Nano Lett.* **2010,** *10,* 4890–4896

during cooling from the growth temperature. These observations suggest that graphene−Cu falls toward the weak end of the spectrum of graphene−metal interactions.

The Cu foil used here had higher purity than the commonly used Alfa Aesar foil (item #13382): 99.999% as opposed to 99.8%.[13] We also grew graphene on the Alfa Aesar foils, but the higher levels of surface impurities or smaller Cu grains prevented useful LEEM imaging. Despite the differing surface quality, the two types of foils have important similarities. First, X-ray diffraction shows that annealed Alfa Aesar foils have the same (100) in-plane texture as the foils we studied. Thus, graphene is growing on Cu(100) crystallographic facets for both foil types. Second, similar graphene island morphologies can be seen in submonolayer films on the Alfa Aesar foil, suggesting that the growth mode is not affected by foil purity (see Supporting Information in ref 13). These mutual properties imply that the behavior observed here is general to graphene on Cu foils.

Graphene is usually grown on Cu foils by chemical vapor deposition (CVD) via methane decomposition. While the results presented here were obtained under ultrahigh vacuum (UHV) growth conditions by the deposition of elemental C, the 4-lobed island morphology observed has also been reported in studies of CVD-grown graphene (see ref 22 and Supporting Material in ref 13).[22] Previous work on the graphene−Ru(0001) system reveals a similar conclusion: the growth mechanism is the same regardless of the C source with no dependence on the details of hydrocarbon decomposition.[11] The occurrence of this four-lobed island morphology is also evidence that the UHV conditions used here, as opposed to the much higher CVD pressures, did not alter the growth behavior. Thus, we expect the growth framework we discuss in this paper to apply to CVD growth of graphene on Cu foils.

We find that graphene films on Cu are prone to be polycrystalline because multiple graphene crystals of different orientations are simultaneously nucleated at individual sites, leading to the four-lobed islands. Furthermore, the graphene is not precisely oriented with respect to the Cu. Despite this, graphene film quality may well be improved through the use of cleaner Cu foils that offer fewer nucleation sites for graphene islands, resulting in fewer grain boundaries. It would also be advantageous to control the type of nucleation event the graphene undergoes to induce individual islands to be monocrystalline.

The graphene film structure may be enhanced through careful attention to the deposition rate of C, although this factor represents a complex balance. A lower C deposition rate is desirable to limit graphene island nucleation density, but it also requires the Cu substrate to be at the growth temperature with partial graphene coverage for a longer time. This will lead to additional Cu surface roughening through localized sublimation, which may be accommodated by defects within the graphene film. Optimizing the deposition rate of C with regards to these two influences will allow for graphene films composed of larger grains with less structural disorder resulting from substrate roughness.

In summary, we report observing graphene growth on polycrystalline Cu foils. Using LEEM and LEED we find that the Cu foils have a pronounced (100) texture after annealing. The graphene islands nucleate heterogeneously, develop a four-lobed shape, and are not single crystals. Instead each lobe is an individual graphene crystal differently oriented on the Cu grain. The curious morphology of these lobes results from a growth mode dominated by edge kinetics with an angularly dependent growth velocity. The fast growth direction is not in a high-symmetry direction of the graphene. This complex interplay between orientation and growth is quite different from observations on other metal surfaces. Efforts to improve the quality of graphene grown on Cu foils must take into account these film evolution processes.

Acknowledgment. The authors thank J. T. Robinson for helpful comments. This work was supported by the Director, Office of Science, Office of Basic Energy Sciences, Division of Materials Sciences and Engineering, of the U.S. Department of Energy under Contract No. De-Ac02−05Ch11231 (Lawrence Berkeley National Laboratory) and Contract No. De-Ac04−94AL85000 (Sandia National Laboratories). J.M.W. acknowledges support from the NSF Graduate Research Fellowship Program.

Supporting Information Available. Raman spectrum of graphene while still supported on the Cu substrate (Figure S1) and LEEM movie of graphene growing on Cu and LEEM movie of graphene growing on Cu. This material is available free of charge via the Internet at http://pubs.acs.org.

REFERENCES AND NOTES

(1) Geim, A. K.; Novoselov, K. S. *Nat. Mater.* **2007**, *6*, 183–191.
(2) Novoselov, K. S.; Jiang, Z.; Zhang, Y.; Morozov, S. V.; Stormer, H. L.; Zeitler, U.; Maan, J. C.; Boebinge, G. S.; Kim, P.; Geim, A. K. *Science* **2007**, *315*, 1379–1379.
(3) Bolotin, K. I.; Sikes, K. J.; Hone, J.; Stormer, H. L.; Kim, P. *Phys. Rev. Lett.* **2008**, *101*, No. 096802.
(4) Novoselov, K. S.; Geim, A. K.; Morozov, S. V.; Jiang, D.; Zhang, Y.; Dubonos, S. V.; Grigorieva, I. V.; Firsov, A. A. *Science* **2004**, *306*, 666–669.
(5) de Heer, W. A.; Berger, C.; Wu, X.; First, P. N.; Conrad, E. H.; Li, X.; Li, T.; Sprinkle, M.; Hass, J.; Sadowski, M. L.; Potemski, M.; Martinez, G. *Solid State Commun.* **2007**, *143*, 92–100.
(6) Rutter, G. M.; Crain, J. N.; Li, T.; First, P. N.; Stroscio, J. A. *Science* **2007**, *317*, 519–522.
(7) Rollings, E.; Gweon, G.-H.; Zhou, S. Y.; Mun, B. S.; McChesney, J. L.; Hussain, B. S.; Federov, A. V.; First, P. N.; de Heer, W. A.; Lanzara, A. *J. Phys. Chem. Solids* **2006**, *67*, 2172–2177.
(8) Sutter, P. W.; Flege, J.-I.; Sutter, E. A. *Nat. Mater.* **2008**, *7*, 406–411.
(9) Yu, Q.; Lian, J.; Siriponglert, S.; Li, H.; Chen, Y. P.; Pei, S.-S. *Appl. Phys. Lett.* **2008**, *93*, 113103.
(10) McCarty, K. F.; Feibelman, P. J.; Loginova, E.; Bartelt, N. C. *Carbon* **2009**, *47*, 1806–1813.
(11) Loginova, E.; Bartelt, N. C.; Feibelman, P. J.; McCarty, K. F. *New J. Phys.* **2009**, *11*, No. 063046.

DOI: 10.1021/nl102788f | *Nano Lett.* **2010,** *10,* 4890–4896

(12) N'Diaye, A. T.; Bleikamp, S.; Feibelman, P. J.; Michely, T. *Phys. Rev. Lett.* **2006**, *97*, 215501.
(13) Li, X. S.; Cai, W. W.; An, J. H.; Kim, S.; Nah, J.; Yang, D. X.; Piner, R. D.; Velamakanni, A.; Jung, I.; Tutuc, E.; Banerjee, S. K.; Colombo, L.; Ruoff, R. S. *Science* **2009**, *324*, 1312–1314.
(14) Li, X.; Cai, W.; Colombo, L.; Ruoff, R. S. *Nano Lett.* **2009**, *9*, 4268–4272.
(15) Barrett, C. S.; Massalski, T. B. *Structure of Metals*; McGraw-Hill: Elmsford, NY, 1980.
(16) Herring, C. *Phys. Rev. Lett.* **1951**, *82*, 87–93.
(17) Frank, F. C. In *Proceedings of an International Conference on Crystal Growth, Cooperstown, NY*; Doremus, R. H., Roberts, B. W., Turnbull, D., Eds.; Wiley: New York, 1958; pp 411−419.
(18) Kim, K. S.; Zhao, Y.; Jang, H.; Lee, S. Y.; Kim, J. M.; Kim, K. S.; Ahn, J. H.; Kim, P.; Choi, J. Y.; Hong, B. H. *Nature* **2009**, *457*, 706–710.
(19) Loginova, E.; Bartelt, N. C.; Feibelman, P. J.; McCarty, K. F. *New J. Phys.* **2008**, *10*, No. 093026.
(20) Preobrajenski, A. B.; Ng, M. L.; Vinogradov, A. S.; Martensson, N. *Phys. Rev. B* **2008**, *78*, No. 073401.
(21) Lee, V.; Park, C.; Jaye, C.; Fischer, D. A.; Yu, Q.; Wu, W.; Liu, Z.; Bao, J.; Pei, S. S.; Smith, C.; Lysaght, P.; Banerjee, S. *J. Phys. Chem. Lett.* **2010**, *1*, 1247–1253.
(22) Colombo, L.; Li, X.; Han, B.; Magnuson, C.; Cai, W.; Zhu, Y.; Ruoff, R. S. *ECS Trans.* **2010**, *28*, 109–114.

DOI: 10.1021/nl102788f | *Nano Lett.* **2010,** *10,* 4890–-4896